

# Modeling the evolution of intrathermocline lenses in the Atlantic Ocean

by B. N. Filyushkin<sup>1</sup> and M. A. Sokolovskiy<sup>2,3</sup>

## ABSTRACT

The existence of a tongue of Mediterranean Water (MW) at the depths of 500–1500 m is a characteristic feature of the hydrological regime in the northeastern part of the Atlantic Ocean. Anticyclonic eddies filled with MW (meddies or lenses) are observed in this region. They are identified via their high temperature and salinity anomalies, which compensate in density, yielding nearly homogeneous meddy cores. The analysis of historical observations has showed that approximately 100 lenses can exist simultaneously in this part of the ocean. High concentration of large water volumes ( $>4000 \text{ km}^3$  each) can be found both in the region of their origin near the Iberian Peninsula and near the Azores Frontal Zone. The latter is precisely the region in which merging of eddies can occur to form larger lenses. The existence of long-living lenses at large distances from the region of their formation is an indirect indication of the fact that merging of lenses occurs (MESOPOLYGON lens, SM1 lens in the SEMAPHORE experiment, and a lens in the Sargasso Sea).

Here, we analyze the results of model experiments on interaction between two anticyclonic eddies applying the contour dynamics method (CDM) to a three-layer ocean. In these experiments, the vertical distribution of layerwise density in the layers, the horizontal size of the eddies (assumed to be cylindrical structures), and their depth location correspond to the observed conditions in the Atlantic Ocean. We show that the evolution of intrathermocline eddies and the evolution of barotropic eddies differ significantly. We found the behavior of interacting eddies in the middle layer depends on the Froude number. We determined the critical distances between the lenses when their merger begins and the destruction<sup>1</sup> criterion for the elliptical intrathermocline eddies.

## 1. Introduction

Mediterranean Water (MW) occupies a significant part of the North Atlantic at depths from 500 to 1500 m. Mediterranean Water that is transported to the ocean by the bottom current through the Strait of Gibraltar is marked by higher temperature and salinity than in the surrounding waters. Anticyclonic eddies of Mediterranean Water (meddies or lenses) are frequently found in the water column of this water mass over the entire scope of its spreading (Swallow, 1969; Armi and Zenk, 1984; Bower *et al.*, 2002; Richardson *et al.*, 1999; Filyushkin *et al.*, 2007).

1. P. P. Shirshov Institute of Oceanology, Russian Academy of Sciences, Moscow, Russia.

2. Water Problems Institute, Russian Academy of Sciences, Moscow, Russia.

3. Corresponding author. *email: sokol@aqu.laser.ru*

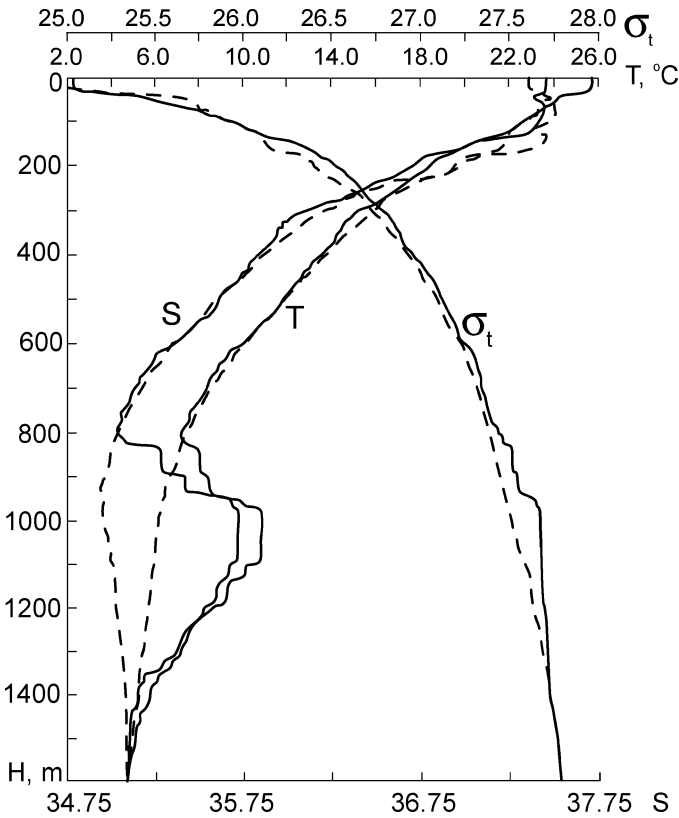


Figure 1. Vertical distributions of temperature, salinity, and density in the center of the MESOPOLYGON lens (solid lines) and background region (dashed lines) (Ivanov *et al.*, 1988).

The lenses are approximately ellipsoidal, with horizontal axes from 40 to 100 km and vertical axes from 0.4 to 1 km and filled with MW. They are characterized by anticyclonic rotation, and their volume can reach  $4000 \text{ km}^3$  (the mean value for the 178 lenses is  $1723 \text{ km}^3$  (Filyushkin *et al.*, 2002b)). Owing to the fact that they are filled with MW, they have high values of temperature and salinity.

Figure 1 shows the vertical distributions of temperature, salinity, and density in the center of the MESOPOLYGON lens and in the background region (Ivanov *et al.*, 1988). The differences between the lens core and the surrounding waters can vary from  $1^\circ$  to  $4^\circ\text{C}$  in temperature and from 0.3 to 1.0 in salinity depending on the distance of the lens from the region of its formation (Filyushkin *et al.*, 2007). The temperature and salinity anomalies nearly compensate to form a homogeneous density. Indeed, the vertical density profiles in the surrounding waters and in the lens center are close, while the core is distinguished for density homogeneity. However, the absolute values of specific density in the lens cores vary

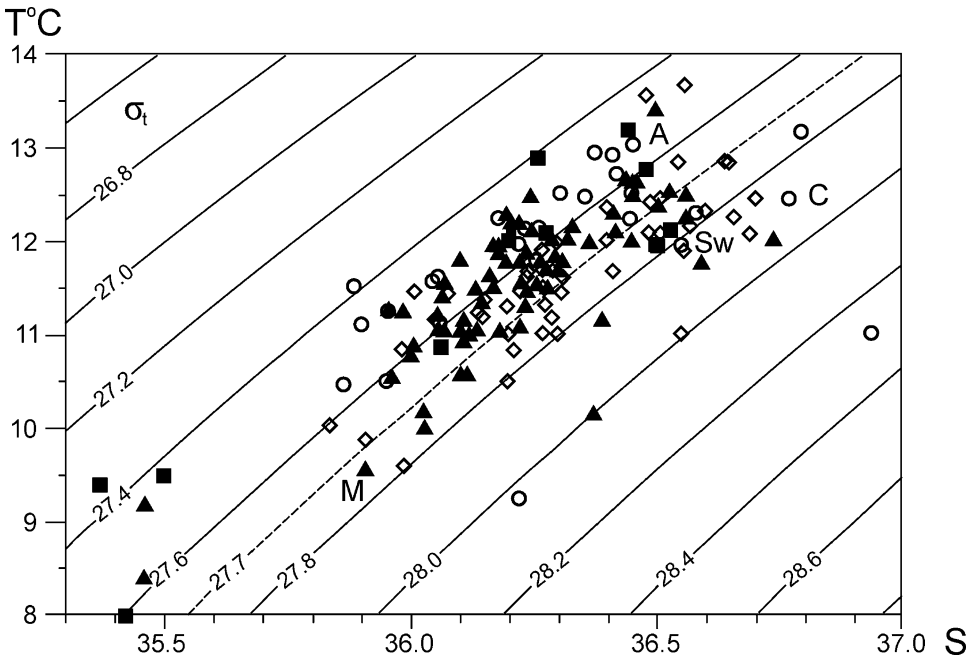


Figure 2. T-S diagram for maximum values temperature and salinity in the lens cores. Depth of the cores: ■ < 800 m; ○ 800–1000 m; ▲ 1000–1200 m; ◇ > 1200 m Sw Cadiz Gulf (Swallow, 1969); M Tropical Atlantic (Yegorikhin *et al.*, 1987); C Cadiz Gulf (Aleynik *et al.*, 1998); A Azores Frontal Zone (Aleynik *et al.*, 1998).

in the range from 27.5 to 28.0, and the lens cores are located at depths from 800 to 1400 m (Filyushkin *et al.*, 2009).

Figure 2 shows a T/S-diagram for the maximum values of temperature and salinity in the meddy cores based on the data catalogue for the period 1968–2007 (Filyushkin *et al.*, 2009). The variability range for these characteristics is related to the different regions and mechanisms of the meddy formation. The long-term measurements show that the main regions of lens formation are the canyons of the Gulf of Cadiz (Swallow, 1969; Armi and Zenk, 1984; Aleynik *et al.*, 1998; Chèrubin *et al.*, 2000; Johnson *et al.*, 2002), the region of Cape Saint Vincent (Schultz Tokos *et al.*, 1994; Richardson *et al.*, 1999; Serra *et al.*, 2002), canyons of the continental slope and western coast of the Iberian Peninsula (Bower *et al.*, 1995; 2002) as well as the region near Cape Ortegal (Paillet *et al.*, 1999; 2002).

Direct observations in the expedition onboard the R/V *Vityaz* (a CTD survey and 9 moorings, Aleynik *et al.*, 1998) at the mouth of the Portimao Canyon showed that during the period from August 12 to 22, 1988, a dipole of anticyclonic and cyclonic eddies formed at depths of 800–1200 m. The anticyclonic lens was displaced by 50 km to the west, and it was investigated in September, 1988 during the expedition onboard the R/V *Oceanus* (Prater,

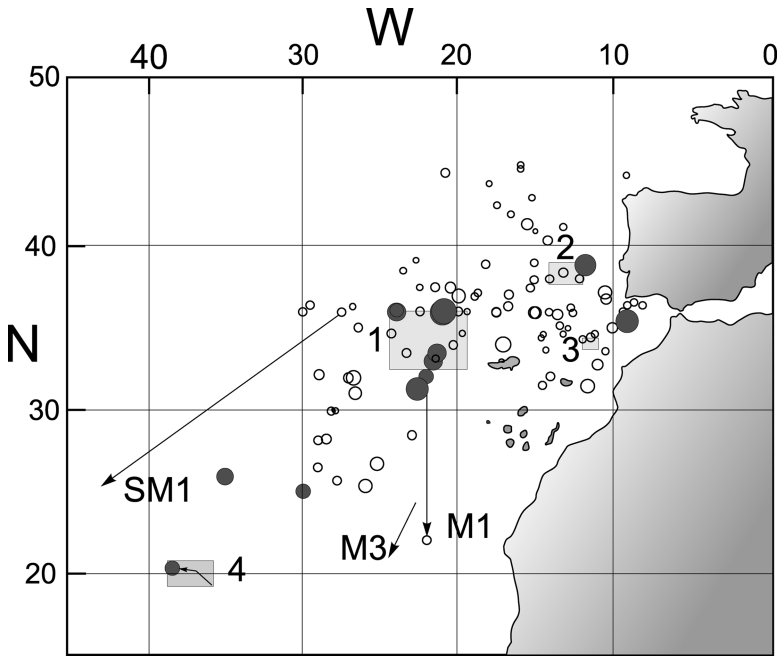


Figure 3. Distribution of Mediterranean lenses in the North Atlantic by the value of their volume (the size of the symbol is proportional to the lens volume, see the text). Dark color highlights the largest lenses. **1** the region of the Azores Frontal Zone (Käse and Zenk 1987; Richardson and Tychensky, 1998; Tychensky and Carton 1998); **2** region of merging of two lenses (Schultz Tokos *et al.*, 1994; Richardson *et al.*, 2000); **3** region of formation of a dipole lens system (Filyushkin, 1989); **4** Mesopolygon (Yegorikhin *et al.*, 1987), SM1 is lens trajectory in the SEMAPHORE study region; M1, M3 are Sharon lens trajectories (Richardson *et al.*, 1989). This figure is an update of the one shown earlier by Filyushkin *et al.* (2002a).

1992). In addition, the fact formation of a dipole system of intrathermocline eddies was observed in the open ocean at a distance of 270 km from the coast of Portugal (Filyushkin and Plakhin, 1996, see also Fig. 3). Two CTD-surveys were carried out from July 6 to 10, 1988 and revealed a clearly pronounced jet of MW (approximately 6-km wide measured at the 36.6 isohaline). The velocity in the inflow jet measured on the mooring at a depth of 1248 m reached  $40 \text{ cm s}^{-1}$ . An asymmetric dipole of eddies was found during the survey on July 22–26, 1988. The anticyclonic lens was significantly larger than the cyclonic one in volume and had two vertically separated cores at depths of 800 and 1200 m. The cyclonic lens had smaller geometrical size and lower salinity in the core. The cyclonic lenses do not travel far because they collapse under destabilizing action of the horizontal surplus pressure gradient, centrifugal, and Coriolis forces. During the same time interval, an anticyclonic lens was found at a distance of 90 km to the south and this lens was studied. It had one core at a depth of 1200 m; no cyclonic lens was found nearby (Filyushkin, 1989). The rapid

destruction of cyclonic lenses determines properties of the MW near its source. At the same time, the main transport of heat and salt at intermediate depths over large distances from the source of their formation (up to 5000 km) is determined by the propagation and destruction of meddies (Armi and Stommel, 1983; Richardson *et al.*, 1989). The meddies, precisely, provide the existence of the intermediate Mediterranean water mass over vast areas of the North Atlantic.

The total number of lenses existing in the ocean simultaneously, the quantity of annually formed lenses, and the lenses lifetimes remain poorly understood. The experimental study of meddies is limited in space and time. For example, Armi and Zenk (1984) estimate that eddies cover from 4 to 8% of the Canary Basin square. Close estimates of the number of lenses in the region of the Azores Frontal Zone were obtained during the experiments POSEIDON (Käse and Zenk, 1987) and SEMAPHORE (Richardson and Tychensky, 1998; Tychensky and Carton, 1998). In each of these experiments, 4 to 6 lenses were found. Nineteen lenses were found within the AMUSE Project during the period from May, 1993 to February, 1994 using the RAFOS floats (Richardson *et al.*, 1999). It was estimated, that 15–20 meddies per year are formed along the Portuguese continental slope, namely between Cape Saint Vincent and Estremadura Promontory (Bower *et al.*, 2002). Some meddies originate offshore of the northwestern corner of Spain (Paillet *et al.*, 1999). Two anticyclonic lenses were found and the formation of two dipolar structures was investigated during the expedition onboard the R/V *Vityaz* from May to September 1988 in the Gulf of Cadiz and south along the Morocco coast (Filyushkin, 1989). These observations have shown that only 15–20 days are needed for the formation of a pair of vortices (cyclone-anticyclone). It is possible to assume that such vortex formations occur many times during a year so that 25–30 meddies per year may form. Although, during twenty years (1980–2000) of time series observations from the deep-sea mooring KIEL.276 (position 33°N, 22°W) only 10 meddies passed the mooring. Six meddies were found during the first four years and only four meddies during the remaining 16 years (Siedler *et al.*, 2000).

Extrapolating these estimates over the entire region of meddy spreading, we can calculate that approximately 100 lenses can exist simultaneously in the North Atlantic (Koshlyakov and Panteleev, 1988; Kostyanoy and Belkin, 1989). Despite the deep location of lenses, the meddy signal can now be detected at the ocean surface. Currently, this signal is recorded by the observations from the geophysical satellites (Stammer *et al.*, 1991; Carton *et al.*, 2010). Processing of these data provides us with a more exact answer to the question about the number of meddies in the North Atlantic.

With the observations of different meddy-searching expeditions and with hydrological databases, different authors plotted spatial distribution of lenses (Kostianoy and Belkin, 1989; Richardson *et al.*, 1991, 2000; Richardson and Tychensky, 1998; Filyushkin *et al.*, 2007, 2009). Currently, more than 220 lenses have been found in the North Atlantic basin from 1967 to 2004 (Filyushkin *et al.*, 2009). This sampling is random; however, it is clearly seen that the meddies are distributed extremely nonuniformly. Usually they are located

within the MW tongue. Generally they propagate the westward and southwestward directions (approximately 70% of the lenses), and only 30% drift to the north and northwest over distances up to 2000 km. Actually, the lenses move as floats of neutral density over the isopycnal surfaces corresponding to their mean density which determines their depth location. The lenses with cores located at depths from 1000 to 1300 m dominate (approximately 70%, see Fig. 2). The speed of lens propagation is influenced by baroclinic mean flow which acts as a baroclinic beta effect and bottom topography (Dykhno *et al.*, 1991; Shapiro *et al.*, 1995; Morel and McWilliams, 1997; Thierry and Morel, 1999; Vandermeirsch *et al.*, 2001, 2002, 2003a,b; Filyushkin *et al.*, 2002b). The mean speed of the lens drift is from 0.8 to 1.4 miles per day. This corresponds to a lifetime of 3–4 years on average. Lens Sharon M1 according to the estimate by Richardson and Tychensky (1998) disintegrated in 4.3 years. The data analyzed here show that approximately 90% of the lenses exist not more than three years and only the remaining 10% live more than 4–5 years.

The spatial distribution of lenses as function of water volume is shown in Figure 3 (Filyushkin *et al.*, 2002a). Distributions of isopycnal anomalies of potential temperature and salinity were calculated to plot this chart. The values of temperature 0.4°C and salinity 0.1 were assumed as the boundary criterion of the minimum anomaly, within which the isopycnal characteristics of the lens were calculated (Koshlyakov and Panteleev, 1988; Richardson *et al.*, 1991; Aleynik, 1998). The size of the symbols in the figure is proportional to the lens volume within the isopycnal salinity anomaly  $S > 0.1$ . The mean value of the volume is  $V = 1723 \text{ km}^3$  average over 178 lenses (Filyushkin *et al.*, 2002a).

The analysis of this chart shows that a high concentration of lenses is found in the region of Cape Saint Vincent and north of the Azores Frontal Zone (Fig. 3, region 1). Lenses of large volumes were found precisely in these two regions: in the first region, a large lens west of the Iberian Peninsula (Schultz Tokos *et al.*, 1994; Richardson *et al.*, 2000), when complete merger of two anticyclonic eddies was found. The most interesting fact is the appearance of large volume lenses at a distance of 1700 km from the region of their formation. Experiments POSEIDON (Käse and Zenk, 1987) and SEMAPHORE (Richardson and Tychensky, 1998; Tychensky and Carton, 1998) were performed in this region. Two eddies separated by a weak meander of the Azores Current were found in the first experiment and the eddies began to approach each other. In the second experiment, a large lens was found that propagated to the southwest. We note that the existence of large eddies in the open ocean at distances up to 2000 km from the region of their formation indicates the possibility of a significant increase in their lifetime (up to 6–7 years) and they can drift over distances around 7000 km. Lens SM1 in the SEMAPHORE experiment (July 1993–January 1995) is such an example. The lens was located at depths of 600–1400 m and the temperature and salinity anomalies at a depth of 1250 m were as large as 4.1°C and 1.1, respectively (Richardson and Tychensky, 1998). During 540 days from the moment of its first record, the lens propagated over a distance of 1700 km with a high drift velocity equal to  $3.9 \text{ cm s}^{-1}$ . It was lost when it crossed the Mid-Atlantic Ridge (Fig. 3). Another lens with a volume of approximately  $4000 \text{ km}^3$  was found and investigated in this region (Aleynik, 1998).

During the MESOPOLYGON experiment from April to June, 1985, a lens was investigated in the tropical Atlantic (20°N, 37°W) at depths of 800–1200 m with a diameter of about 70 km and temperature and salinity anomalies reaching 4°C and 1.0, respectively (Ivanov *et al.*, 1988).

Finally, in 1976, a lens with a diameter of approximately 100 km was found in the southwestern part of the Sargasso Sea (25°N, 69°W) at depths between 600 and 1300 m. The temperature and salinity anomalies were 2° and 0.4 relative to the surrounding waters (McDowell and Rossby, 1978). Lenses of lesser size were also found in this region, but the values of temperature and salinity below the main thermocline were high (Vinogradov and Pavel'son, 1980; Dugan *et al.*, 1982).

The long-living lenses located to the southwest of the Azores Frontal Zone allow us to confirm indirectly the merger of anticyclonic eddies at large distances from the region of their formation.

In this paper we consider the results of model experiments related to different aspects of the interaction between two anticyclonic eddies applying the contour dynamics method (CDM) to the model three-layer ocean. The vertical distribution of density in the layers, the sizes of eddies, and their depth locations correspond to the actually observed conditions in the Atlantic Ocean.

## 2. Three-layer quasi-geostrophic model of the ocean

Let us consider a three-layer model of the ocean with homogeneous densities in the layers and nonzero thicknesses of the layers<sup>4</sup>. The conservation laws are valid in each of the layers in the quasi-geostrophic approximation in the absence of external forcing

$$\frac{d_j \Pi_j}{dt} = 0, \quad j = 1, 2, 3$$

for components  $\Pi_j$  of a three-dimensional vector of potential vorticity  $\mathbf{\Pi}$ . The vorticity  $\mathbf{\Pi}$  is coupled with the corresponding perturbation vector of the hydrostatic pressure (relative to the pressure in the state of hydrostatic equilibrium) in the rigid lid approximation at the upper surface of the upper layer by a linear differential operator

$$\mathbf{\Pi} = \nabla^2 \mathbf{p} + \mathbf{A} \mathbf{p},$$

$$\mathbf{\Pi} = \begin{pmatrix} \Pi_1 \\ \Pi_2 \\ \Pi_3 \end{pmatrix}, \quad \mathbf{p} = \begin{pmatrix} p_1 \\ p_2 \\ p_3 \end{pmatrix}, \quad \mathbf{A} = \begin{pmatrix} -F_1/h_1 & F_1/h_1 & 0 \\ F_1/h_2 & -(F_1 + F_2)/h_2 & F_2/h_2 \\ 0 & F_2/h_3 & -F_2/h_3 \end{pmatrix}, \quad (1)$$

where  $F_n = \rho_0 (fL)^2 / (g \Delta \rho_n H)$ ,  $\Delta \rho_n = \rho_{n+1} - \rho_n$ ,  $n = 1, 2$ . Here,  $\rho_j$  ( $j = 1, 2, 3$ ) are fluid densities in the layers (numerated from top down),  $H = h(h_1 + h_2 + h_3)$  is

4. For the first time, the idea to use a three-layer model for describing the lens dynamics was formulated by Hogg and Stommel (1990). See also (Carton *et al.*, 2010).

the total depth ( $h$  is its scale, so that for the dimensionless thicknesses of layers  $h_j$  we get  $h_1 + h_2 + h_3 = 1$ ),  $L$  is the horizontal scale,  $g$  is acceleration due to gravity,  $f$  is the Coriolis parameter assumed constant,  $\rho_0$  is the mean density of the fluid,  $\nabla^2 \equiv \partial^2/\partial x^2 + \partial^2/\partial y^2$  and  $d_j/dt = \partial/\partial t - (\partial p_j/\partial y)\partial/\partial x + (\partial p_j/\partial x)\partial/\partial y$ .

Using the method of diagonalization described in Kamenkovich *et al.* (1982), reduces (1) to system

$$\Phi = \nabla^2 \varphi + D\varphi, \tag{2}$$

where  $p = Q\varphi$ ,  $\Phi = S\Pi$ ,  $D = \lambda_j E$ ,

$$Q = (\mathbf{q}^{(1)}, \mathbf{q}^{(2)}, \mathbf{q}^{(3)})$$

$$= \begin{pmatrix} 1 & \frac{h_3 \lambda_3}{\lambda_3 - \lambda_2} & -\frac{F_1}{h_1 \lambda_3} \\ 1 & \frac{h_3 \lambda_3 + F_2/h_2}{\lambda_3 - \lambda_2} & -\left(\frac{F_1}{h_1 \lambda_3} + 1\right) \\ 1 & \frac{h_3 \lambda_3 + F_2/h_2 + \lambda_2 + F_1(h_1 + h_2)/h_1 h_2}{\lambda_3 - \lambda_2} & -\left(\frac{F_1}{h_1 \lambda_3} + 1 + \frac{h_2(\lambda_3 + F_1(h_1 + h_2)/h_1 h_2)}{F_2}\right) \end{pmatrix}$$

$$S = Q^{-1}$$

$$= \begin{pmatrix} h_1 & h_2 & h_3 \\ -\frac{h_2(\lambda_3 + F_1(h_1 + h_2)/h_1 h_2)}{F_2} & \frac{h_2(\lambda_3 + (F_1(h_1 + h_2) + F_2 h_1)/h_1 h_2)}{F_2} & -1 \\ -\frac{\lambda_2 + F_1(h_1 + h_2)/h_1 h_2}{\lambda_3 - \lambda_2} & \frac{\lambda_2 + (F_1(h_1 + h_2) + F_2 h_1)/h_1 h_2}{\lambda_3 - \lambda_2} & -\frac{F_2/h_2}{\lambda_3 - \lambda_2} \end{pmatrix},$$

$$\lambda_1 = 0, \quad \lambda_{2,3} = -\frac{1}{2} \sqrt{\frac{F_1}{h_1} + \frac{F_1 + F_2}{h_2} + \frac{F_2}{h_3} \mp \left( \left( \frac{F_1}{h_1} + \frac{F_1 + F_2}{h_2} + \frac{F_2}{h_3} \right)^2 - 4 \frac{F_1 F_2}{h_1 h_2 h_3} \right)},$$

$\lambda_j$  are eigenvalues of the spectral problem  $A\mathbf{q} + \lambda\mathbf{q} = 0$ ;  $\mathbf{q}^{(1)}, \mathbf{q}^{(2)}, \mathbf{q}^{(3)}$  are its eigenvectors,  $E$  is a unit matrix.

Components  $\varphi_j$  of the auxiliary vector  $\varphi$  can be determined using the Green's function  $G_j$ :

$$\varphi_j = \iint_{-\infty}^{+\infty} \Phi_j G_j(r) dx_1 dy_1, \quad j = 1, 2, 3,$$

$$G_j(r) = \frac{1}{2\pi} \begin{cases} \ln r, & j = 1, \\ -K_0(\gamma_1 r), & j = 2, \\ -K_0(\gamma_2 r), & j = 3, \end{cases}$$

where  $K_0$  is modified Bessel function of zero order (below the notations  $K_1$  and  $I_1$  will be used for the modified Bessel functions of the first order),  $r = \sqrt{(x - x_1)^2 + (y - y_1)^2}$ ,  $\gamma_{1,2} = \sqrt{-\lambda_{2,3}}$ . The pressures in the layers are convenient to represent using the regular functions  $\tilde{G}_1 = G_2 - G_1$ ,  $\tilde{G}_2 = G_3 - G_1$ , and  $G_1$  which has an integrated singularity at  $r \rightarrow 0$ :  $p_j = \int_{-\infty}^{+\infty} [\Pi_j G_1 + q_{j2}(s_{21}\Pi_1 + s_{22}\Pi_2 + s_{23}\Pi_3)\tilde{G}_1 + q_{j3}(s_{31}\Pi_1 + s_{32}\Pi_2 +$

$s_{33}\Pi_3)\tilde{G}_2]dx_1dy_1$ , where  $q_{jl}$  and  $s_{jl}$  ( $j, l = 1, 2, 3$ ) are elements of the matrices  $Q$  and  $S$  introduced above. Assuming  $\Pi_j$  to be piecewise constant functions of the form  $\Pi_j = \sum_{m=1}^{m_j} \Pi_{jm}$  with constant values of  $\Pi_{jm}$  on compact supports  $\sigma_{jm}$ , and using the Stokes theorem for a transition to contour integrals we get

$$\begin{aligned}
 p_j = & \sum_{m=1}^{m_j} \Pi_{jm} \oint_{c_{jm}} W w dv_{jm} + q_{j2} \sum_{n=1}^3 s_{2n} \sum_{m=1}^{m_n} \Pi_{nm} \oint_{c_{nm}} W_1 w dv_{nm} \\
 & + q_{j3} \sum_{n=1}^3 s_{3n} \sum_{m=1}^{m_n} \Pi_{nm} \oint_{c_{nm}} W_2 w dv_{nm}, \quad j = 1, 2, 3, \tag{3}
 \end{aligned}$$

where  $C_{jl}$  are contours of domains  $\sigma_{jl}$  described with the continuously varying parameter  $v_{jl}$  in the domain,

$$\begin{aligned}
 W = & \frac{r^2}{4\pi} \left( \ln r - \frac{1}{2} \right), \quad W_{1,2} = \frac{1}{2\pi\gamma_{1,2}} (\gamma_{1,2} r K_1(\gamma_{1,2} r) - 1) - W, \\
 w = & \frac{(x_1 - x)\dot{y}_1 - (y_1 - y)\dot{x}_1}{r^2},
 \end{aligned}$$

the dot superscript represents differentiation with respect to  $v_{jl}$ .

Now we select a set of  $N_{jm}$  reference points on each contour  $C_{jm}$ , and can write equations of motion

$$\begin{aligned}
 \frac{dr_n^{(jm)}}{dt} = & V_n^{(jm)}, \\
 r_n^{(jm)}|_{t=0} = & r_{n0}^{(jm)}, \quad n = 1, 2, \dots, N_{jm}, \quad m = 1, 2, \dots, m_j, \quad j = 1, 2, 3, \tag{4}
 \end{aligned}$$

where  $r_n^{(jm)}$  is radius vector of  $n$ th Lagrange particle of contour  $C_{jm}$  bounding the vortex patch  $m$  in the layer  $j$ . The right parts of Eqs. (4) are determined from (3) using geostrophic relations. It is clear that they are related by means of contour integrals, which allows us to use the version of contour dynamics method (Kozlov, 1983) generalized to the case of three-layer rotating fluid by Sokolovskiy (1991).

Ordinary differential equations (4) with corresponding initial conditions were solved using the Runge-Kutta method of the fourth order and time step equal to  $\Delta t = 0.05$ , while the numerical integration, differentiation, and interpolation over grid functions determining contours  $C_{jm}$ , were performed using the method of periodical cubic splines (Kozlov, 1983). Programming codes for contour dynamics and contour surgery developed by Makarov (1990, 1991) were used in the calculations.

### 3. A model of intrathermocline lenses

It is known from oceanographic observations (Ivanov *et al.*, 1988) that intrathermocline eddies are usually identified by the anomalous values of temperature and salinity and almost

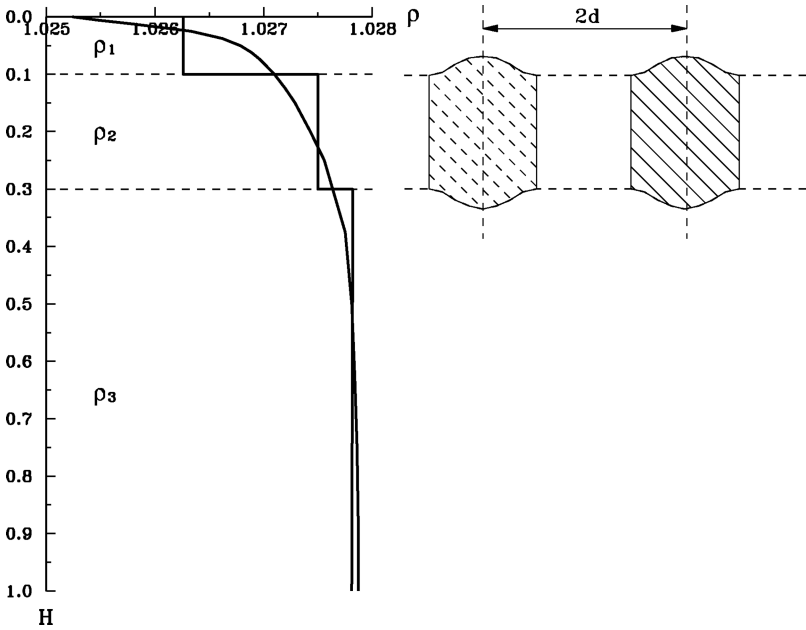


Figure 4. Schematic presentation of a three-layer model and two anticyclonic lenses (the vertical coordinate axis is strongly stretched).

do not differ in density from the surrounding water masses in the horizontal direction. This is a motivation for using a three-layer quasi-geostrophic model with eddy patches located in the middle layer to construct an adequate model of oceanic eddies. In this case, owing to the geostrophic balance, anticyclonic (cyclonic) eddies in the middle layer have a form of double-convex (double concave) lenses.

We specify the geophysical parameters in the model taking into account the realistic long-term average density profiles in the Atlantic (Kamenkovich *et al.*, 1986) (smooth solid line in the left part of Fig. 4) and mean horizontal scales of the eddies (Yegorikhin *et al.*, 1987). The vertical density distribution is approximated by a two-step piecewise constant function with density jumps at the interface boundaries between the layers  $\Delta\rho_1 = \rho_2 - \rho_1$  and  $\Delta\rho_2 = \rho_3 - \rho_2$ , so that  $\Delta\rho_1/\Delta\rho_2 = 4$ , and dimensionless thicknesses of the layers are  $h_1 = 0.1$ ,  $h_2 = 0.2$ , and  $h_3 = 0.7$ . If we assume such relation between the thicknesses of the layers and ocean depth equal to 5000 m, the middle layer would occupy the layer between 500 and 1500 m. Two density jumps are naturally associated with two Froude numbers  $F_n$  ( $n = 1, 2$ ) introduced above. Using notation  $F \equiv F_1$  we get  $F_2 = 4F$ .

The following considerations motivate the choice of these parameters. In the work (Sokolovskiy *et al.*, 2001), it is shown that use of the Flierl (1978) method for calibrating the two-layer model of the Atlantic (the layers densities are  $\rho_1$  and  $\rho_2$ , and their nondimensional thicknesses are  $h_1$  and  $h_2$ ) gives  $h_1 = 0.095$  and  $\Delta\rho = \rho_2 - \rho_1 = 2.63 \times 10^{-3}\rho_0$ ; where

$\rho_0$  being the mean density. So, for our calculations we can assume  $h_1 = 0.1$ . The value of  $h_2$  equal to 0.2 was chosen for modeling MW in the layer 500–1500 m. The suggestion  $\Delta p_1/\Delta p_2 = 4$ , i.e.  $F_2 = 4F$  satisfies such relation of depths exactly.

#### 4. Non-stationary dynamics of lenses in three-layer model

We consider two related problems: (1) interaction of two circular eddy patches and (2) evolution of an elliptical eddy patch. In both cases we assume that the eddies are located only in the middle layer. Hence, they are prototypes of the Atlantic lenses.

##### *a. Merger of circular vortices*

It is known (Lamb, 1932) that two point vortices equal in magnitudes and signs rotate with a constant angular velocity relative to the center of the segment connecting these vortices in the sense determined by the sign of the vortices. Two identical distributed circular vortices behave similarly if they are located sufficiently far from each other (Hopfinger and van Heijst, 1993), but they can merge when they are sufficiently close to each other. The problem of merger of vortices of the same sign in a homogeneous or two-layer fluid (plasma) is one of the fundamental problems in hydrodynamics and many publications are dedicated to this problem (Christiansen and Zabusky, 1973; Winant and Browand, 1974; Takaki and Kovaznay, 1978; Overman and Zabusky, 1982; Freymuth *et al.*, 1984, 1985; Nof and Simon, 1987; Griffiths and Hopfinger 1987; Melander *et al.*, 1987, 1988; Cushman-Roisin, 1989; Dewar and Killworth, 1990; Carnevale *et al.*, 1991; Fine *et al.*, 1991; Carton, 1992; Waugh, 1992; Hopfinger and van Heijst, 1993; Valcke and Verron, 1993a,b; 1996; Verron and Valcke, 1994; Morel and Carton, 1994; Yasuda, 1995; Yasuda and Flierl, 1995, 1997; Lansky *et al.*, 1997; Polvani, 1988; Lumpkin *et al.*, 2000; Marcus *et al.*, 2000; Sokolovskiy and Verron, 2000; Velasco Fuentes, 2001; Meunier and Leweke, 2001; Amoretti *et al.*, 2001, 2002; Carton *et al.* 2002; Meunier *et al.*, 2002; Dritschel, 2002; Renaud and Dritschel, 2002, 2005; Le Dizés and Verga, 2002; Cerretelli and Williamson, 2003; Huang, 2005; Ferreira de Sousa and Pereira, 2005; Brandt and Nomura 2006; Brandt *et al.*, 2010).

The key problem is the estimation of the critical distance between the centers of the vortices at which the merging process manifests itself. It was found that two cylindrical circular eddies of a unit radii merge if  $d < d^* \approx 1.7$ , where  $d$  is half distance between the eddy centers (see the right part of Fig. 4) (Hopfinger and van Heijst, 1993; Velasco Fuentes, 2001). We note that these results for the critical value  $d^*$  were obtained for vortex patches (vortices with constant distribution of vorticity) in a barotropic fluid. In the case considered here, the eddy patches of unit radius in the middle layer are located between two “free” interface surfaces, which play a principal role according to the calculations.

The interval for  $d^* \in [1.69, 1.71]$  (Fig. 5a) obtained from CDM-calculations is limited in the barotropic case by two vertical dashed lines. To the left of the left line (domain  $M$ ) the vortex patches always merge, while to the right of the right line they do not merge (domain

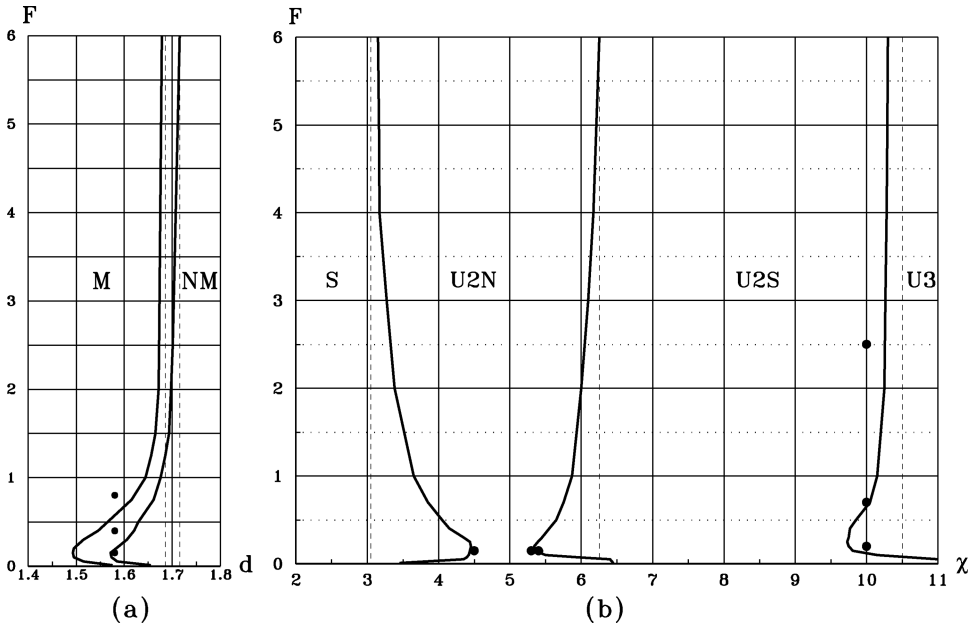


Figure 5. A diagram of different states: (a) two circular eddy patches on the surface of parameters ( $d$ ,  $F$ ) in a barotropic fluid (dashed lines) and in the middle layer of a three-layer fluid (solid lines); (b) the same for one elliptical eddy on the parameter plane ( $\chi$ ,  $F$ ). The dots correspond to the coordinates of the plane of indicated parameters, for which the numerical experiments shown in Figures 6–9 (a) and Figures 10–15 (b) were performed.

*NM*). Within a narrow interval between them either a one-time merger with subsequent separation is observed or this event is repeated many times.

In the three-layer case the corresponding boundaries are not constant and are functions of  $F$  (solid lines): at large values of  $F$ , the barotropic limit is reached while in the interval of variation of parameter  $F$  from 0 to approximately 1.5, the distribution by parameter  $F$  is nonmonotonic with a minimum at  $F \approx 0.15$ . Assuming, for example, that,  $f = 10^{-4} \text{ s}^{-1}$ ,  $g = 10^2 \text{ g cm}^3 \text{ s}^{-2}$ ,  $\rho_0 = 1 \text{ g cm}^{-3}$ ,  $H = 5 \cdot 10^5 \text{ cm}$ ,  $\Delta\rho_1 = \frac{4}{5} \cdot \Delta\rho = 2.1 \cdot 10^{-3} \text{ g cm}^{-3}$  and  $F = 0.15$ , we get that the characteristic radius of the vortices which are the least subject to merger is  $L = 3.96 \cdot 10^6 \text{ cm} = 39.6 \text{ km}$ .

Figures 6–9 present the results of modeling calculations of the evolution of two equal circular eddies with unit radii, located in the middle layer, at the same initial distance between their centers, but at different values of parameter  $F$  (three dark markers in Fig. 5a).

Figure 6 presents an example of the behavior of lenses located close to each other ( $d = 1.58$ ) at  $F = 0.15$  (lower marker in Fig. 5a), when the vortex patches rotate relatively to

5. We note that such effect was observed in the laboratory experiments by Griffiths and Hopfinger (1987) during the merging of two eddies of the upper layer in a two-layer fluid. See also (Polvani, 1988; Carton, 2001).

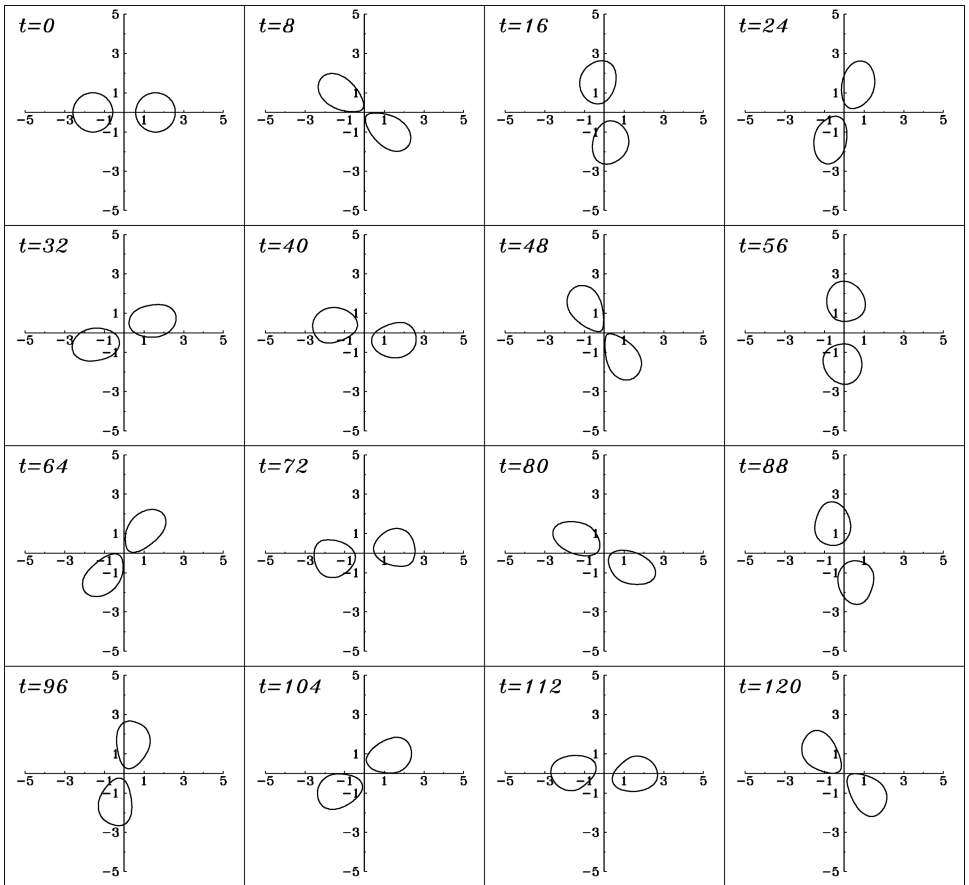


Figure 6. Motion of initially circular eddies in the middle layer without merging:  $F = 0.15$ ,  $d = 1.58$ .

their mid point without merger. The figure shows that in this case, the vortex patches move toward and then away from each other similarly to the observed interaction of the Aska meddies B1 and B2 (Schultz Tokos *et al.*, 1994).

Figure 7, where  $F = 0.40$  (middle marker in Fig. 5a), illustrates the process of multiple merger and further separation of the vortex patches. In particular, this example gives one of the possible explanations of the frequently observed chaotic process in the behavior of the neutral buoyancy floats: such floats initially localized in one of the circular vortex patches and later (after merger and separation) appear in the same vortex as well as in the other vortex, and this action can be repeated.

Figure 8 gives the visualization of the mixing process during merger and splitting of vortex patches; one of the initially circular lenses being dyed. In this picture, we can see how mixing occurs. In particular, it demonstrates that the fluid, initially located in one of the vortices, is distributed among the vortex patches after the split of the quasi-elliptical vortex.

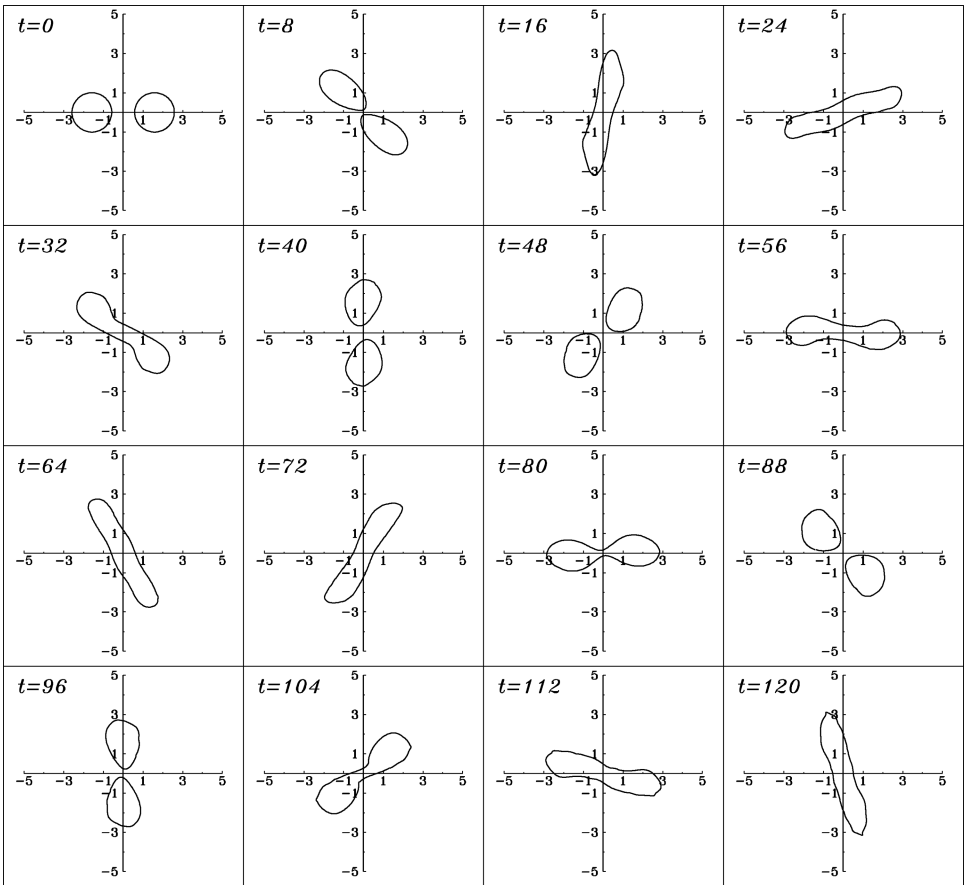


Figure 7. Motion of initially circular eddies in the middle layer with periodical merging and subsequent separation:  $F = 0.4$ ,  $d = 1.58$ .

Figure 9 ( $F = 0.80$  is the lower marker in Fig. 5a) illustrates an example of the case when merger of vortices already occurs at the initial stage of evolution. The vortex structure that appears as the result of the merger of initially circular patches has a form of pulsating quasi-elliptical lens rotating in the anticyclonic direction, surrounded by small-scale vortices that separated during the transition state. After the separation of vortex filaments and small vortices (the role of filamentation in the merger of anticyclonic lenses is investigated in detail by Cushman-Roisin (1989)), the remaining core takes a compact form with the ratio between the half-axes not exceeding 4. Thus, it is stable (see Fig. 5b).

Everywhere, the configurations of the vortex patches are shown at the dimensionless moments. The scaling is such that one dimensionless time unit corresponds to the rotational period, with the fluid velocity equal to  $30 \text{ cm s}^{-1}$  at the vortex radius (Koshlyakov and

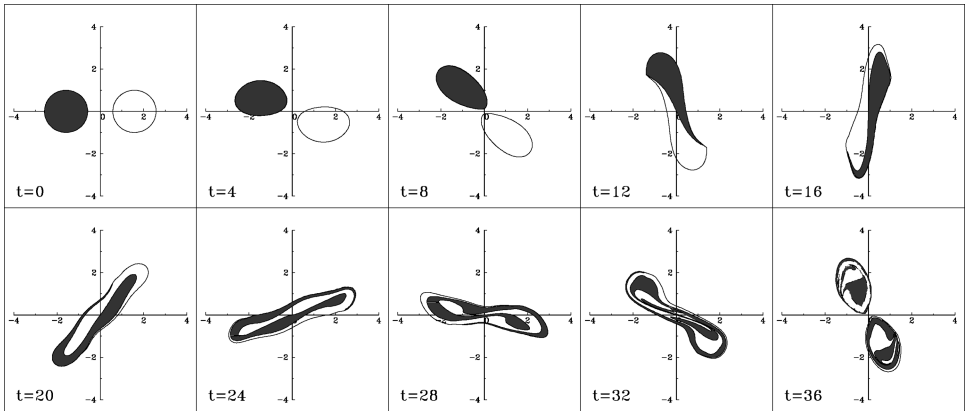


Figure 8. Visualization of the mixing process during merging and splitting of the vortex patches under the conditions of the experiment in Figure 7, i. e. at  $F = 0.4$ ,  $d = 1.58$  (time interval of the results are cut by half).

Pantelev, 1988). Thus, one unit of the dimensionless time corresponds approximately to 10, 16, and 24 days in the first, second, and third cases, respectively.

### *b. Evolution of elliptical vortices*

The classical Kirchhoff solution (Kirchhoff, 1876) of the elliptical vortex patch with half-axes  $a$  and  $b$  and vorticity  $\omega$ , rotating as a solid body with angular velocity  $\Omega = \omega ab / (a+b)^2$  has been known since 1876. In 17 years, Love (1893) demonstrated that at  $\chi = a/b > 3$  this stationary solution is unstable. Recently, Mitchell and Rossi (2008) presented a complete quantification of the regimes of the linear and nonlinear instability of the elliptical vortex with respect to parameter  $\chi$ .

Here, we investigate the possible scenarios of the evolution of the elliptical vortex patches placed in the middle layer of three-layer fluid, depending on the fluid stratification. Keeping in mind that in the previous series of calculations the quasi-elliptical vortices could be generated as a result of the merger of two circular vortices. We consider the vortex patches with the square equivalent to the squares of two circular vortices; i.e.,  $ab = 2$ .

Results of numerical experiments are summarized in the diagram shown in Figure 5b. The dashed vertical lines represent the boundaries of stability domains in the barotropic case: in the domain  $S$  the elliptical patch is stable, in  $U2N^6$ ,  $U2S$ , and  $U3$  it is unstable with division of the vortex patch into two nonequal parts, into two equal parts, and into three parts, respectively.

6. The asymmetry effect during the destruction of elliptic eddy patches was found for the first time in (Kozlov and Makarov, 1984), where the authors also presented their considerations about inevitability of asymmetry at  $3.3 < \chi < 6.5$ ; see also (Brandt *et al.*, 2010).

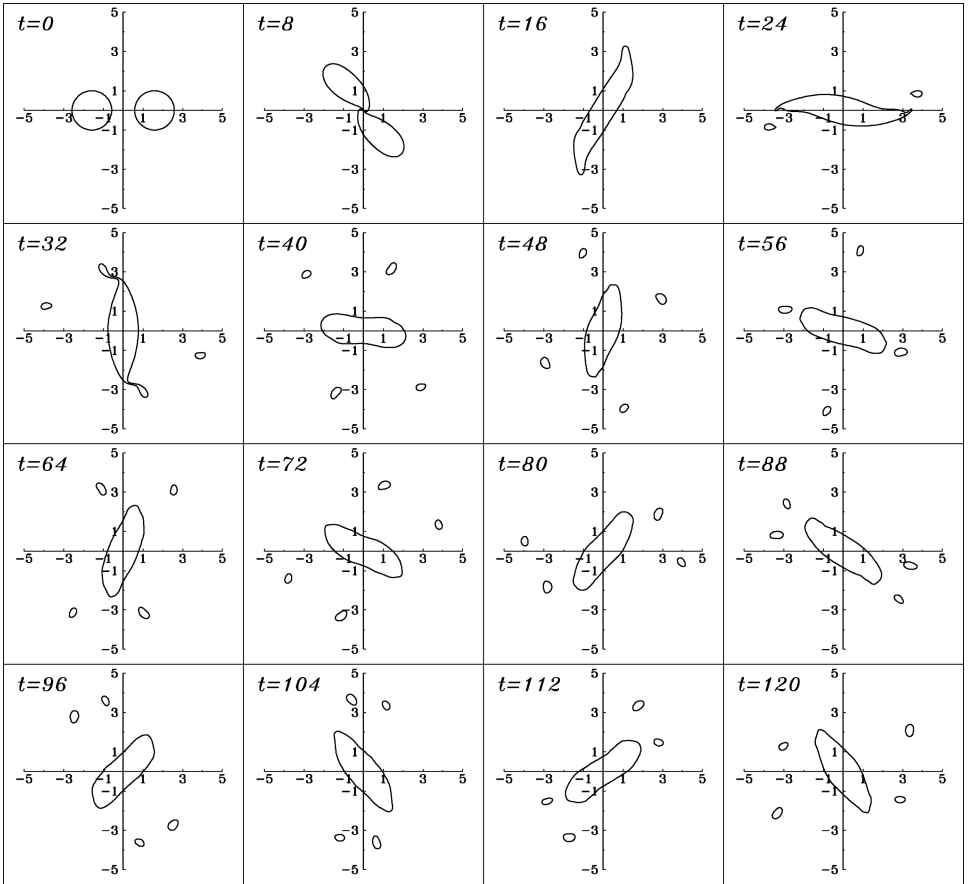


Figure 9. Motion of initially circular eddies in the middle layer with merging:  $F = 0.8, d = 1.58$ .

The thick solid lines show the corresponding boundaries for the elliptical lenses. Like in the case of merger of vortices, behavior of the boundaries between the regimes is nonmonotonic with respect to parameter  $F$ . It is worth noting that extreme properties are observed at the same critical value  $F \approx 0.15$ ; on the one hand this value corresponds to the most favorable stability conditions for the elliptical vortex patch (up to  $\chi \approx 4.4$ ), on the other hand, the interval in which the conditions of asymmetric division of the vortex are satisfied is minimal with respect to parameter  $\chi$ .

Figures 10 and 11, where  $\chi \approx 4.5$  and  $\chi \approx 5.4$ , respectively, give examples of the behavior of the vortex patch for  $F = 0.15$  and limiting extreme values of the ellipse eccentricity. In the first case, the vortex patch is stable for a long time and only at  $t > 200$  does it begin to manifest the asymmetry property and then divide into two unequal parts. In the second case, before the final disintegration into two parts of different size, it splits three

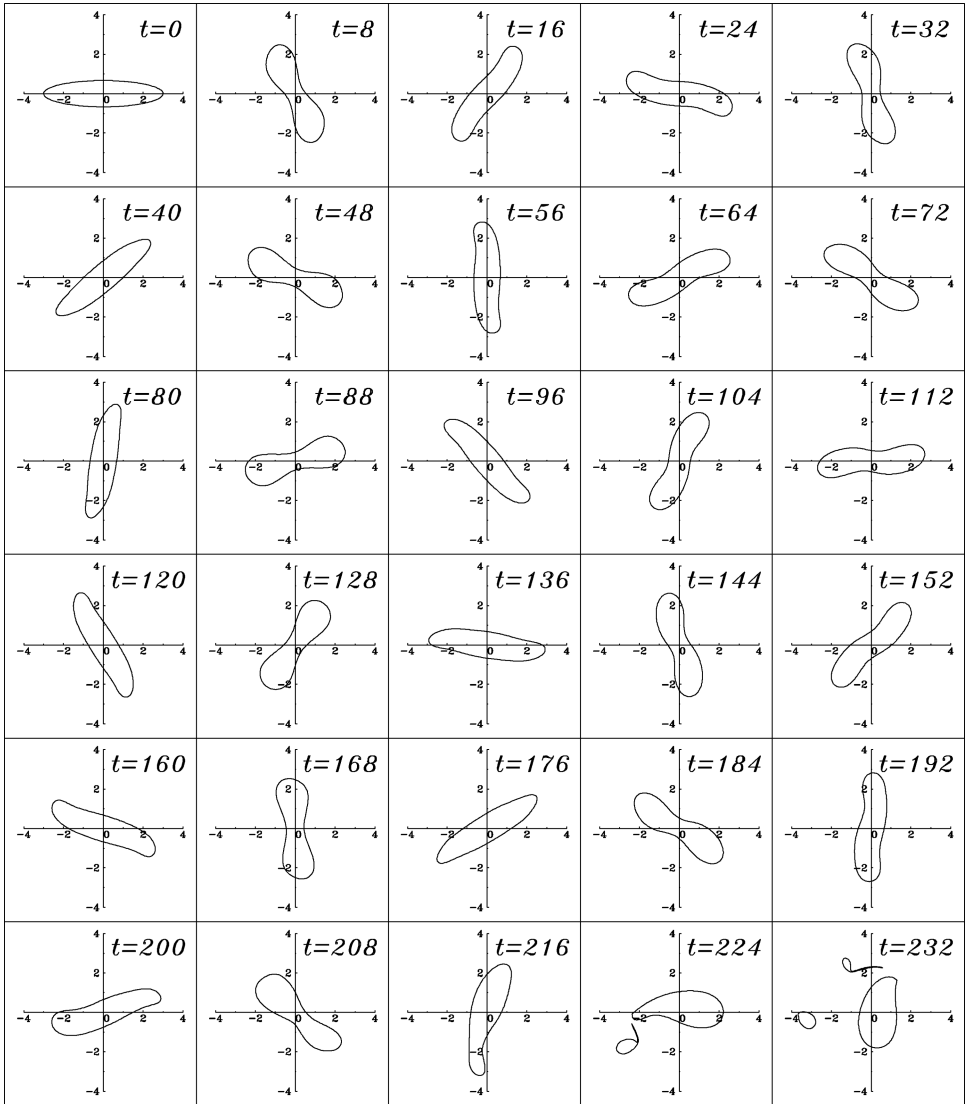


Figure 10. Evolution of a lens of elliptical shape at  $F = 0.15$ ,  $\chi = 4.5$  (division into asymmetrical parts and separation of small eddies).

times into nearly equal parts, which merge again into one single connected structure. If parameter  $\chi$  increases by 0.1 (Fig. 12), the disintegration into two equal quasi-circular parts becomes irreversible. This corresponds to the result of the experiment shown in Figure 6 representing the possibility of an anomalous coming together of two circular vortices without merger at  $F = 0.15$ .

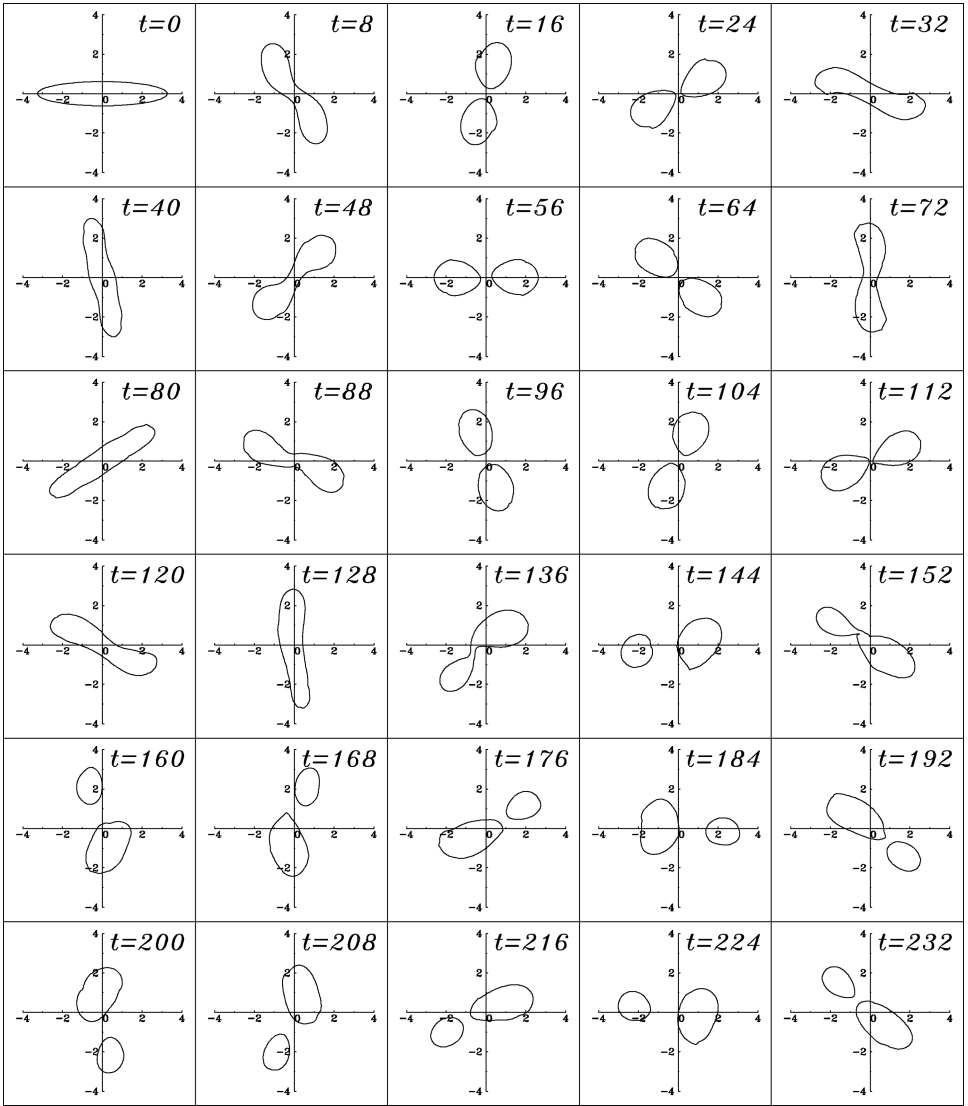


Figure 11. Evolution of a lens of elliptical shape at  $F = 0.15$ ,  $\chi = 5.3$  (division into asymmetrical parts).

The next three figures demonstrate the behavior of elliptic vortex at  $\chi = 10$  and different values of  $F$ . Such a strongly elongated configuration can serve, for example, as a model of the Mediterranean salt tongue investigated in Spall *et al.*, 1993.

A tendency to the formation of the third mode is seen in Figure 13 where  $F = 2.5$ . This occurs at relatively weak stratification when marker in Figure 5b belongs to domain

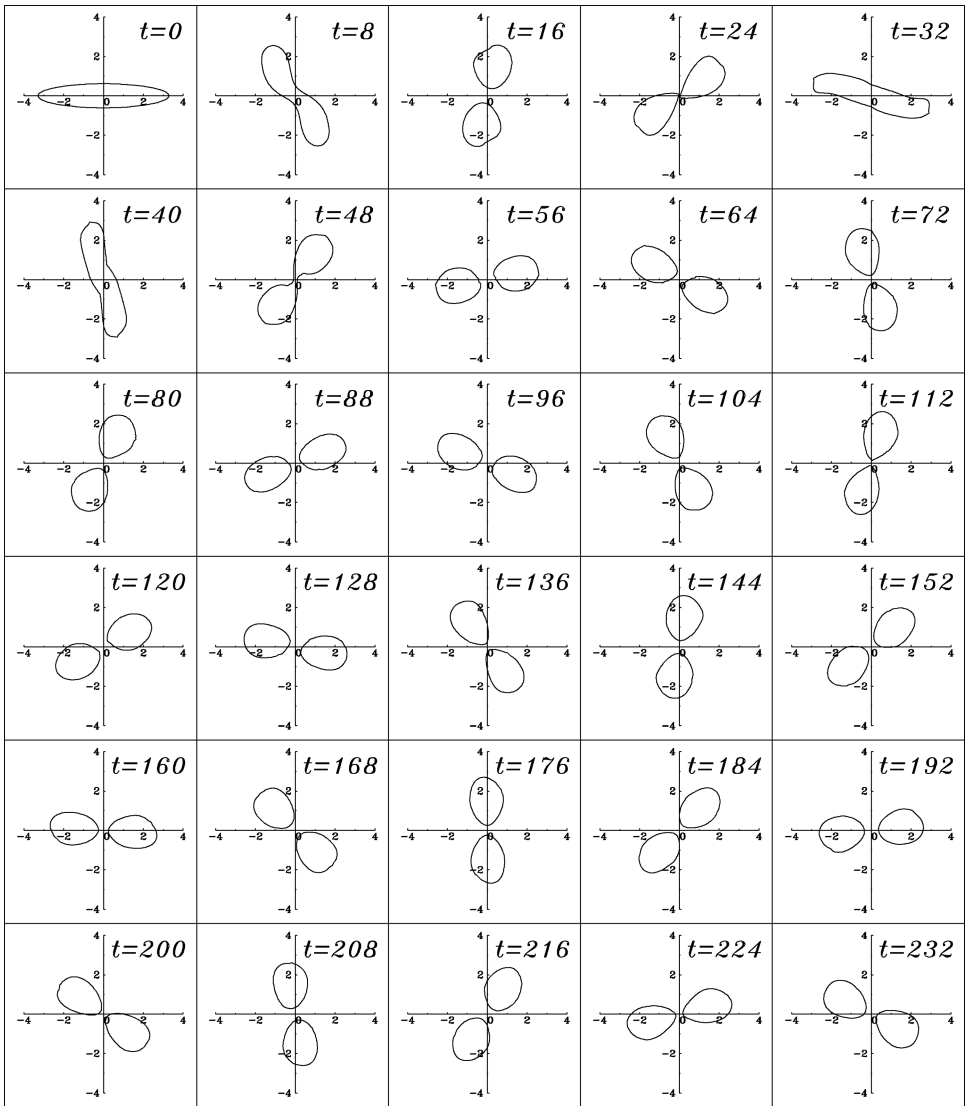


Figure 12. Evolution of a lens of elliptical shape at  $F = 0.15$ ,  $\chi = 5.4$  (division into symmetrical parts).

$U2S$ , at the intermediate stage (approximately  $t \in [12, 24]$ ). Later the central thickening is stretched into a filament, which results in the formation of the symmetric second mode. We note that the barotropic elliptical patches behave similarly (Kozlov and Makarov, 1984).

The influence of the third mode is much stronger and can be seen in Figure 14 where  $F = 0.7$ , and the marker in Figure 5b is already very close to the boundary with domain

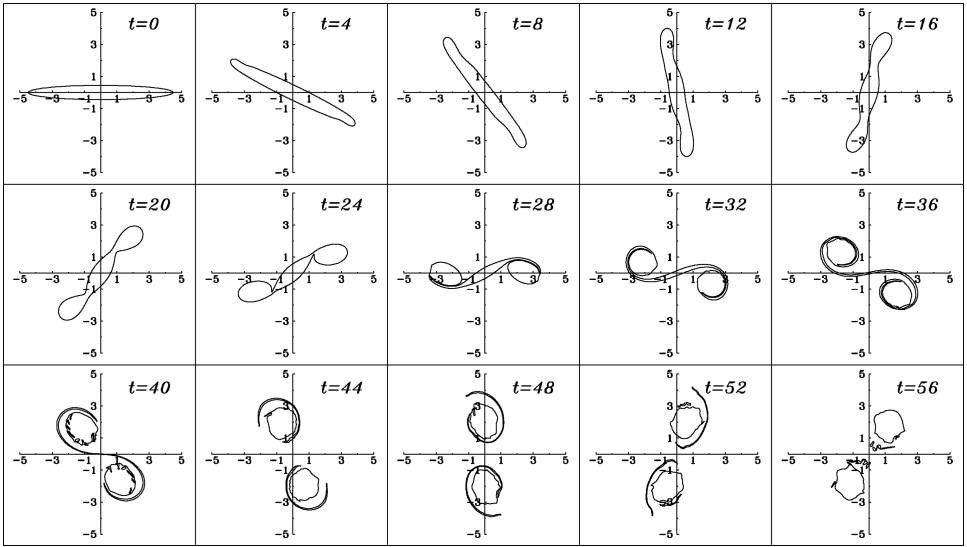


Figure 13. Evolution of a lens of elliptical shape at  $F = 2.5$ ,  $\chi = 10$  (symmetrical division during the realization of the second mode).

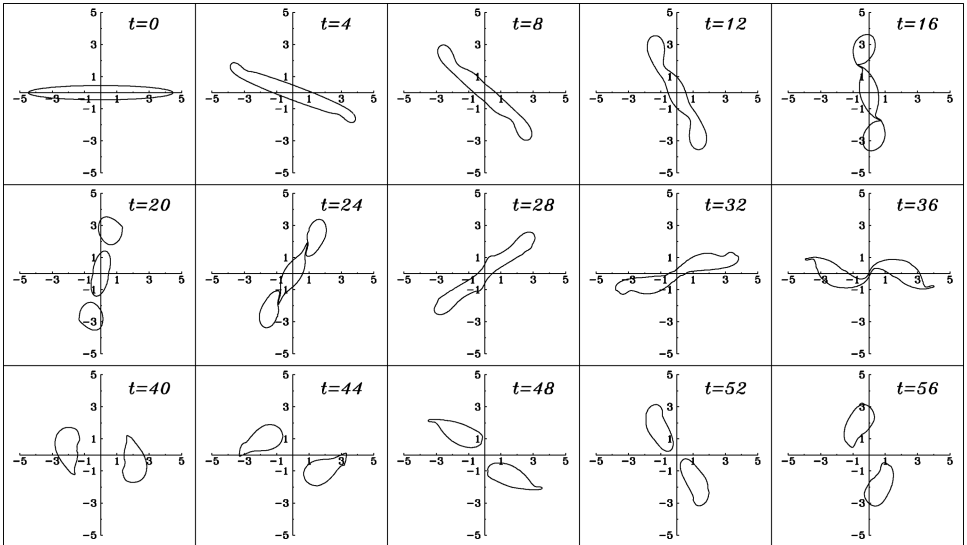


Figure 14. Evolution of a lens of elliptical shape at  $F = 0.7$ ,  $\chi = 10$  (sequential formation of the third mode, merging and separation into two parts).

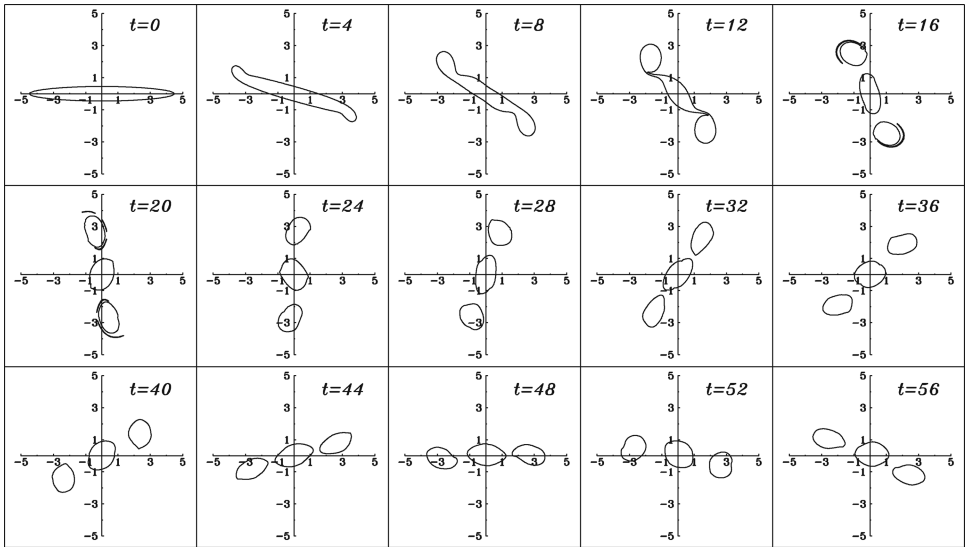


Figure 15. Evolution of a lens of elliptical shape at  $F = 0.2$ ,  $\chi = 10$  (formation of the third mode).

$U3$ . At time  $t = 20$ , we actually observe the disintegration of the vortex into three parts, but then they merge again, and eventually the mode two is realized.

Figure 15 shows an example of the third mode formation at  $F = 0.2$ . For a given duration, this three-pole structure is quite stable (at least at  $t \in [16, 56]$  which corresponds to the interval more than one year in dimension coordinates; but after a long time it disintegrates due to instability<sup>7</sup>. It is noteworthy that in the barotropic case the corresponding point on the plane  $(\chi, F)$  is related to domain  $U2S$ , which is seen in Figure 5b.

Thus, the results of numerical experiments presented here demonstrate that intrathermocline lenses modeling as vortex patches in the middle layer of a three-layer rotating fluid behave in many aspects similarly to the barotropic vortices, but for moderate and strong stratification, the criteria of merger of circular vortices and behavior of elliptical vortices change significantly. In this case, the Froude number or, in other words, the ratio of the characteristic size of the vortex structure to the Rossby deformation radius is added to the main parameters characterizing the bifurcations of the dynamic regimes such as relative closeness of the vortex patches in the first case and the eccentricity of the ellipse in the second case.

## 5. Conclusion

The meddies are distinguishable by their high temperature and salinity values but in their cores the water is approximately homogeneous in density. This makes the meddies a special

7. It should be noted that the analogous structure consisting of three point vortices having practically the same intensity is unstable.

class of eddies in the ocean. It is possible to determine their location in the ocean as well as their geometric sizes, heat and salt content, available potential energy, and investigate their variability in time at all stages of their life up to the complete degradation.

All meddies are located in the intermediate waters layer 500–1500 m deep. To simplify the problem we represent the ocean as a three-layer fluid with constant densities, and assume that the potential vorticity of the model meddies is confined to the middle layer. The densities and the layer depths are specified taking into account realistic stratification in the Atlantic and horizontal scales of the meddies. Therefore, the results of the model experiments can be compared with the observed eddies in the ocean.

Similar to the barotropic case, merging of the vortices occurs when the distance between their centers is less than a critical distance  $d^*$ . In the barotropic case  $d^* \approx 1.7$  for the vortices of unit radii. In our case,  $d^*$  is a nonmonotonic function of the Froude number  $F$ . At small  $F$  the distance  $d^*$  is close to 1.7, then it decreases with increasing  $F$  reaching the minimum  $d^* \approx 1.57$  at  $F \approx 0.15$  and tends to 1.7 with further increasing  $F$ . Thus, at  $F \approx 0.15$ , circular lenses may uniformly rotate about a common center of vorticity without merging, being at the minimum distance from each other. The same value of the Froude number plays an important role in dynamics of lenses having the elliptical shape. First, it corresponds to the conditions of maximum stability of an elliptic vortex patch having the ratio of the semi-axes up to  $\chi = 4.4$  versus  $\chi = 3$  for the barotropic case. Second, when  $F \approx 0.15$ , we have a minimum interval with respect to  $\chi$  of the area of the asymmetric bipartition of an elliptic vortex ( $4.4 < \chi < 5.3$  versus  $3 < \chi < 6.5$ ), and, in addition, the most favorable conditions for the formation of an unstable symmetric second mode ( $5.3 < \chi < 9.7$  versus  $6.5 < \chi < 10.5$ ) and of a third one ( $\chi > 9.7$  versus  $\chi > 10.5$ ).

In conclusion we emphasize two important points. Despite the fact that the lens cores are localized at the intermediate depth far away from the surface, they influence dynamically the entire water column in the ocean; hence indirect visual observation of lenses can also be performed from satellites (Stammer *et al.*, 1991). This is confirmed theoretically. As mentioned above, an anticyclonic eddy takes the form of double convex lens owing to the geostrophic balance. Local deformations of the interface surfaces, in their turn induce anticyclonic relative vorticity in the upper and the lower layers due to the invariance of the potential vorticity (Filyushkin *et al.*, 2011). For a circular lens with  $\Pi_1 = \Pi_3 = 0$ ,  $\Pi_2 = \Pi$ , the azimuthal velocity of fluid particles is given by equations

$$V_j(r) = \Pi \sum_{n=1}^3 q_{jn} \sum_{m=1}^3 s_{nm} E_{m-1}(r), \quad j = 1, 2, 3, \tag{5}$$

where

$$E_0(r) = \frac{1}{2} \begin{cases} r, & r \leq 1, \\ 1/r, & r > 1, \end{cases} \quad E_i(r) = \begin{cases} \mathbf{K}_1(\gamma_i) \mathbf{I}_1(\gamma_i r), & r \leq 1, \\ \mathbf{K}_1(\gamma_i r) \mathbf{I}_1(\gamma_i), & r > 1, \end{cases} \quad i = 1, 2.$$

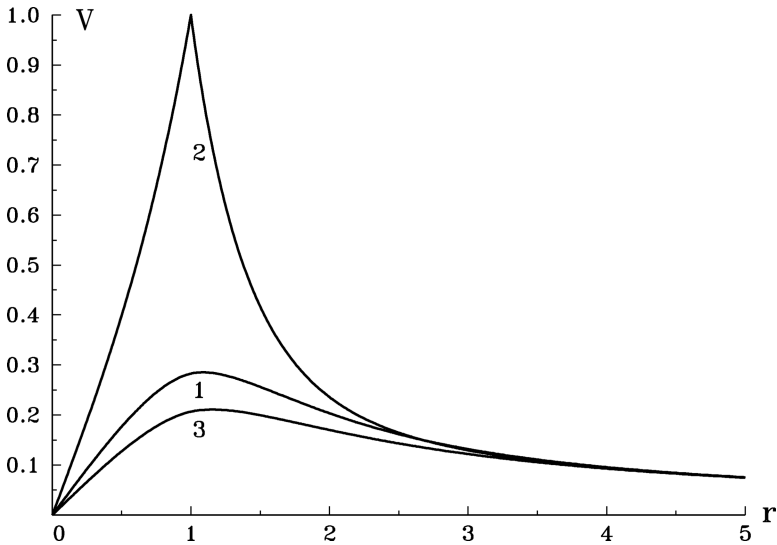


Figure 16. Normalized profiles of the azimuthal velocities in the upper (1), middle (2) and lower (3) layers induced by a circular anticyclonic lens of a unit radius belonging to the middle layer calculated using relation (5).

Figure 16 demonstrates the behavior of profiles (5) in each of the layers. As for elliptical lenses, Figure 17 shows an example of the streamlines calculated for time moment  $t = 16$  in Figure 14. We see that the vortex flows generated in the upper and lower layers are topologically close to the structures in the middle layer. Thus, these model calculations confirm that detection of lenses in the intermediate layer can be performed using remote observations of the ocean surface. Certainly, confirmation of these theoretical results requires the simultaneous analysis of satellite observations and direct observation from research ships using CTD-surveys, clusters of moorings, and autonomous floats located in the body of the eddy (Carton *et al.*, 2010).

The analysis of experimental observations has demonstrated that MW eddy propagation in the northeastern part of the Atlantic is an important element of hydrological structure of the ocean. Taking into account that the total number can be as large as 100 (Filyushkin *et al.*, 2009), it becomes obvious that the considered mechanisms of anticyclonic lens merger can be helpful in explaining the regularities of the appearance of large-volume intrathermocline eddies in different regions of the ocean. In particular, the appearance of such large lenses in the region of the Azores Frontal Zone allows us to explain the existence of long-living meddies at great distances from this region.

Transport of MW at intermediate depths by individual eddies over large distances during many years can be comparable with the advective transport of heat and salt (Armi and Stommel, 1983; Richardson *et al.*, 1989). Estimates by different researchers indicate that

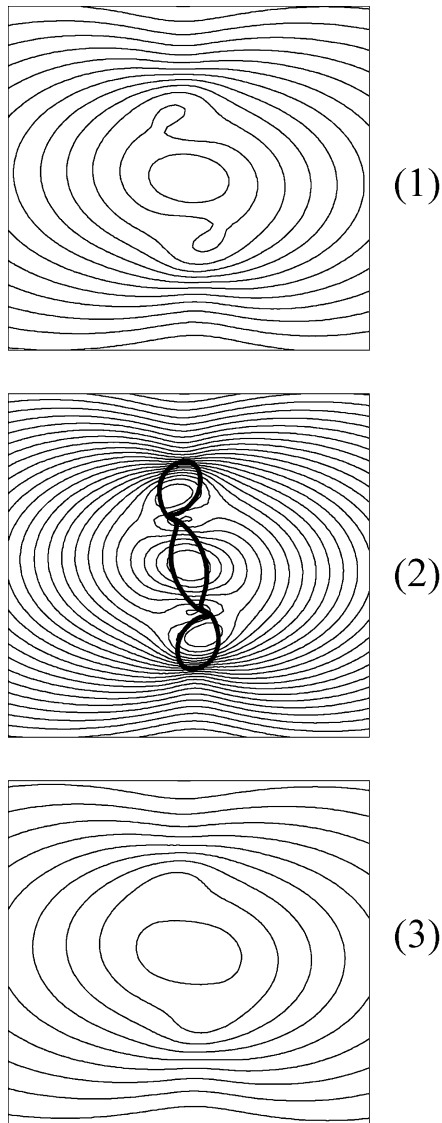


Figure 17. Streamlines of the horizontal motion in the upper (1), middle (2) and lower (3) layers for the case shown in Figure 14 at  $F = 0.7$ ,  $\chi = 10$  at the time  $t = 16$ . The solid line shows the contours of the eddy patches.

the meddies' contribution to the total flux of the salinity anomaly can be substantial. For example, Richardson *et al.* (1989) estimate this contribution as 25%, Arhan *et al.* (1994) as more than 50%, and Mazé *et al.* (1997) as almost 100%. So, we can speak about the climatic role of the long-living eddy transport to maintain of the Mediterranean salt tongue

as prominent hydrographic features of the mid-depth North Atlantic (Wüst, 1935; Bubnov, 1971; Kuksa, 1983).

*Acknowledgments.* The authors would like to thank Dr Gregory Reznik for helpful discussions, the anonymous referees who carefully proofread this paper, and Ms Olga Yakovenko for technical assistance. This study was supported by the Russian Foundation for Basic Research (Projects 09-05-00778, 10-05-00144, 10-05-00432, 10-05-00646, 11-01-12057), RFBR/CNRS (Project 11-05-91052), Ministry of Education of the RF (Project 2.1.1/554).

## REFERENCES

- Aleynik, D. L. 1998. The structure and evolution of a meddy and Azores frontal zone in autumn 1993. *Oceanology*, *38*, 312–322.
- Aleynik, D. L., E. A. Plakhin and B. N. Filyushkin. 1998. On the mechanism of formation of intrathermocline lenses in the canyon area of the Gulf of Cadiz continental slope. *Oceanology*, *38*, 645–653.
- Amoretti, M., D. Durkin, J. Fajans, R. Pozzoli and M. Romé. 2001. Asymmetric vortex merger: Experiments and simulations. *Phys. Plasmas*, *8*, 3865–3868.
- . 2002. Experimental and numerical study of asymmetric vortex merger in a pure electron plasma, *in* Non-Neutral Plasma Physics IV, Anderegg *et al.*, eds., Am. Inst. Physics, 459–463.
- Arhan, M., A. Colin de Verdière and L. Mémerly. 1994. The eastern boundary of the subtropical North Atlantic. *J. Phys. Oceanogr.*, *24*, 1295–1316.
- Armi, L. and H. Stommel. 1983. Four views of a portion of the North Atlantic subtropical gyre. *J. Phys. Oceanogr.*, *13*, 828–857.
- Armi, L. and W. Zenk. 1984. Large lenses of highly saline Mediterranean water. *J. Phys. Oceanogr.*, *14*, 1560–1576.
- Bower, A. S., L. Armi and I. Ambar. 1995. Direct evidence of the meddy formation off south-western coast of Portugal. *Deep-Sea Res.*, *42*, 1621–1630.
- Bower, A. S., N. Serra and I. Ambar. 2002. Structure of the Mediterranean undercurrent and Mediterranean water spreading around the southwestern Iberian Peninsula. *J. Geophys. Res.*, *107*, C10, 3161, doi: [10.1029/2001JC001007](https://doi.org/10.1029/2001JC001007).
- Brandt, L. K., T. K. Cichocki and K. K. Nomura. 2010. Asymmetric vortex merger: mechanism and criterion. *Theor. Comput. Fluid. Dyn.* *24*, 163–167.
- Brandt, L. K. and K. K. Nomura. 2006. The physics of vortex merger: Further insight. *Phys. Fluids*, *18*, 051701, doi: [10.1063/1.2201474](https://doi.org/10.1063/1.2201474).
- Bubnov, V. A. 1971. Structure and dynamics of the Mediterranean waters in the Atlantic Ocean. *Ocean. Res.*, *22*, 220–286 (in Russian).
- Carnevale, G. F., P. Cavazza, P. Orlandi and R. Purini. 1991. An explanation for anomalous vortex merger in rotating-tank experiments. *Phys. Fluids*, *A3*, 1411–1416.
- Carton X. J. 1992. On the merger of shielded vortices. *Europhys. Lett.*, *18*, 697–703.
- . 2001. Hydrodynamical modeling of oceanic vortices. *Surveys in Geophys.*, *22*, 179–263.
- Carton, X., L. Chèrubin, J. Paillet, Y. Morel, A. Serpette and B. Le Cann. 2002. Meddy coupling with a deep cyclone in the Gulf of Cadiz. *J. Marine Syst.*, *32*, 13–42.
- Carton X., N. Daniault, J. Alves, L. Chèrubin and I. Ambar. 2010. Meddy dynamics and interaction with neighboring eddies southwest of Portugal: Observations and modeling. *J. Geophys. Res.*, *115*, C06017, doi: [10.1029/2009JC005646](https://doi.org/10.1029/2009JC005646).

- Carton, X., G. Maze and B. Legras. 2002. A two-dimensional vortex merger in an external strain field. *J. Turbulence*, 3, 1–7.
- Cerretelli, C. and C. H. K. Williamson. 2003. The physical mechanism for vortex merging. *J. Fluid Mech.*, 475, 41–77.
- Chèrubin, L. M., X. Carton, J. Paillet, Y. Morel and A. Serpette. 2000. Instability of the Mediterranean water undercurrents southwest of Portugal: effects of baroclinicity and topography. *Oceanol. Acta*, 23, 551–573.
- Christiansen, J. P. and N. J. Zabusky. 1973. Instability, coalescence and fission of finite-area vortex structures. *J. Fluid Mech.*, 61, 219–273.
- Cushman-Roisin, B. 1989. On the role of filamentation in the merging of anticyclonic lenses. *J. Phys. Oceanogr.*, 19, 253–258.
- Dewar, W. K. and P. D. Killworth. 1990. On the cylinder collapse problem, mixing, and the merger of isolated eddies. *J. Phys. Oceanogr.*, 20, 1563–1575.
- Dritschel, D. G. 2002. Vortex merger in a rotating stratified flows. *J. Fluid Mech.*, 455, 83–101.
- Dugan, J. P., R. P. Mied, P. C. Mignerey and A. P. Schuetz. 1982. Compact, intrathermocline eddies in the Sargasso Sea. *J. Geophys. Res.*, 87, 385–393.
- Dykhnov, L. A., Ye. G. Morozov, S. V. Nikitin, B. N. Filyushkin and I. A. Shilov. 1991. Breakup of lenses of Mediterranean water on interaction with bottom relief. *Oceanology*, 31, 38–41.
- Ferreira de Sousa, P. J. S. A. and J. C. F. Pereira. 2005. Reynolds number dependence of two-dimensional laminar co-rotating merging. *Theor. Comput. Fluid Dyn.*, 19, 65–75.
- Filyushkin, B. N. 1989. Investigation of intrathermocline lenses of Mediterranean origin (Cruise 16 of R/V “Vityaz”, June 3–September 16, 1988). *Oceanology*, 29, 535–536.
- Filyushkin, B. N., D. L. Aleynik, V. M. Gruzinov and N. G. Kozhelupova. 2002a. The thermohaline water structure at the region dynamic degradation of the Mediterranean lenses, *in Proc. State Oceanogr. Inst., “Ocean and Sea Research,”* S-Ptb. No 208, 15–32 (in Russian).
- 2002b. Dynamic degradation of the Mediterranean lenses in the Atlantic Ocean. *Dokl. Earth Sci.*, 387, 1079–1082.
- Filyushkin, B. N., D. L. Aleynik, N. G. Kozhelupova and S. N. Moshonkin. 2009. Horizontal transport peculiarities of the Mediterranean water in the Atlantic, *in Proc. State Oceanogr. Inst., “Ocean and Sea Research,”* Moscow, No 212, 76–88 (in Russian).
- Filyushkin, B. N., A. N. Demidov, A. A. Sarafanov and N. G. Kozhelupova. 2007. The peculiarity of the formation and spreading Mediterranean water mass at intermediate depths of the Atlantic Ocean, *in Waters Masses of the Oceans and Sea*, MAX Press, Moscow, 92–129 (in Russian).
- Filyushkin, B. N. and E. A. Plakhin. 1996. Experimental study of the first stage of Mediterranean water lens formation. *Oceanology*, 35, 797–804.
- Filyushkin, B. N., M. A. Sokolovskiy, N. G. Kozhelupova and I. M. Vagina. 2010. Dynamics of intrathermocline lenses. *Dokl. Earth Sci.*, 434, 1377–1380.
- 2011. Reflection of intrathermocline eddies on the ocean surface. *Dokl. Earth Sci.*, 439 (Part 1), 986–989.
- Fine, K. S., C. F. Driscoll, J. H. Molmberg and T. B. Mitchell. 1991. Measurements of symmetric vortex merger. *Phys. Rev. Lett.*, 67, 588–591.
- Flierl, G. R. 1978. Models of vertical structure and the calibration of two-layer models. *Dyn. Atmos. Oceans*, 2, 341–381.
- Freythuth, P., W. Bank, M. Palmer. 1984. First experimental evidence of vortex splitting. *Phys. Fluids*, 27, 1045–1046.
- 1985. Further experimental evidence of vortex splitting. *J. Fluid Mech.*, 152, 289–299.

- Griffiths, R. W. and E. J. Hopfinger. 1987. Coalescing of geostrophic vortices. *J. Fluid Mech.*, 178, 73–97.
- Hogg, N. G. and H. M. Stommel. 1990. How currents in the upper thermocline could advect meddies deeper down. *Deep-Sea Res.*, 37, 613–623.
- Hopfinger, E. J. and G. J. F. van Heijst. 1993. Vortices in rotating fluids. *Ann. Rev. Fluid Mech.*, 25, 241–289.
- Huang, M.-J. 2005. The physical mechanism of symmetric vortex merger: A new viewpoint. *Phys. Fluids*, 17, 074105, doi: [10.1063/1.1949647](https://doi.org/10.1063/1.1949647).
- Ivanov, Yu. A., V. G. Kort, S. M. Shapovalov and A. D. Sh'erbinin. 1988. Mesoscale intrusion lenses. Proc. Hydrophysical Studies at “Mesopolygon” Program, Moscow, Science, 41–46 (in Russian).
- Johnson, J., L. Ambar, N. Serra and I. Stevens. 2002. Comparative studies of the spreading of Mediterranean water through the Gulf of Cadiz. *Deep-Sea Res. II.*, 49, 4179–4193.
- Kamenkovich, V. M., M. N. Koshlyakov and A. S. Monin. 1986. Synoptic Eddies in the Ocean. V. M. Kamenkovich, ed., Kluwer Academic Publishers, Dordrecht, Holland, 444 pp.
- Kamenkovich, V. M., V. D. Larichev and B. V. Khar'kov. 1982. A numerical barotropic model for analysis of synoptic eddies in the open ocean. *Oceanology*, 21, 549–558.
- Käse, R. H. and W. Zenk. 1987. Reconstructed Mediterranean salt lens trajectories. *J. Phys. Oceanogr.*, 17, 158–161.
- Kirchhoff, G. 1876. Vorlesungen über mathematische Physik: Mechanik. Taubner, Leipzig.
- Koshlyakov, M. N. and G. G. Pantelev. 1988. Thermohaline characteristic of the Mediterranean water lens at tropical zone North Atlantic, in *Hydrophysical research by program Mesopolygon*, Moscow, Nauka, 46–57 (in Russian).
- Kostianoy, A. G. and G. M. Belkin. 1989. A survey of observations on intrathermocline eddies in the world ocean, in *Mesoscale/Synoptic Coherent Structure in Geophysical Turbulence*, J. C. J. Nihoul and B. M. Jamart, eds., Elsevier, 821–841.
- Kozlov, V. F. 1983. The method of contour dynamics in model problems of the ocean topographic cyclogenesis. *Izv., Atmos. Oceanic Phys.*, 19, 635–640.
- Kozlov, V. F. and V. G. Makarov. 1984. Evolution modeling of unstable geostrophic eddies in a barotropic ocean. *Oceanology*, 24, 556–560.
- Kuksa, V. I. 1983. The intermediate waters of the World Ocean. Hydrometeoizdat, Leningrad, 272 pp (in Russian).
- Lamb, H. 1932. *Hydrodynamics* (6th ed), Cambridge University Press, 768 pp.
- Lansky, I. M., T. M. O'Neil and D. A. Schecter. 1997. A theory of vortex merger. *Phys. Rev. Lett.*, 79, 1479–1482.
- Le Dizés, S. and A. Verga. 2002. Viscous interactions of two co-rotating vortices before merging. *J. Fluid Mech.*, 467, 389–410.
- Love, A. E. H. 1893. On the stability of certain vortex motion. *Proc. Lond. Math. Soc.*, 25, 18–42.
- Lumpkin, R., H. Flament, R. Kloosterziel and L. Armi. 2000. Vortex merging in a  $1\frac{1}{2}$ -layer fluid on an  $f$  plane. *J. Phys. Oceanogr.*, 30, 233–242.
- Makarov, V. G. 1990. Set of programs for the investigation of dynamics of two-dimensional vertical motions of inviscid fluid by contour dynamics method, in *Method Contour Dynamics in Oceanic Investigations*, Vladivostok, Far-East Division of Academy of Sciences, 28–39 (in Russian).
- 1991. Computational algorithm of the contour dynamics method with changeable topology of domains under study. *Model. Mech.*, 5, 83–95 (in Russian).
- Marcus, P. S., T. Kundu and C. Lee. 2000. Vortex dynamics and zonal flows. *Phys. Plasmas*, 7, 1630–1640.

- Mazé, J. P., M. Arhan and H. Mercier. 1997. Volume budget of the eastern boundary layer off the Iberian Peninsula. *Deep-Sea Res.*, I, *44*, 1543–1574.
- McDowell, S. E. and H. T. Rossby. 1978. [Mediterranean waters: An intense mesoscale eddy off Bahamas. \*Science\*, 202, 1085–1087.](#)
- Melander, M. V., N. J. Zabusky and J. C. McWilliams. 1987. Asymmetric vortex merger in two dimensions: Which vortex is “victorious”? *Phys. Fluids*, *30*, 2610–2612.
- . 1988. Symmetric vortex merger in two dimensions: causes and conditions. *J. Fluid Mech.*, *195*, 303–340.
- Meunier, P. and T. Leweke. 2001. Three-dimensional instability during vortex merging. *Phys. Fluids*, *13*, 2747–2750.
- Meunier, P., U. Ehrenstein, T. Leweke and M. Rossi. 2002. [A merger criterion for two-dimensional co-rotating vortices. \*Phys. Fluids\*, 14, 2757–2766.](#)
- Mitchell, T. B. and L. F. Rossi. 2008. The evolution of Kirchhoff elliptic vortices. *Phys. Fluids*, *20*, 054103, doi: [10.1063/1.2912991](https://doi.org/10.1063/1.2912991).
- Morel, Y. G. and X. J. Carton. 1994. Multipolar vortices in two-dimensional incompressible flows. *J. Fluid Mech.*, *267*, 23–51.
- Morel, Y. and J. McWilliams. 1997. Evolution of isolated interior vortices in the ocean. *J. Phys. Oceanogr.*, *27*, 727–748.
- Nof, D. and L. M. Simon. 1987. Laboratory experiments on the merging of nonlinear anticyclonic eddies. *J. Phys. Oceanogr.*, *17*, 343–357.
- Overman, E. A. II and N. J. Zabusky. 1982. Evolution and merger of isolated vortex structures. *Phys. Fluids*, *25*, 1297–1305.
- Paillet, J., B. LeCann, X. Carton, Y. Morel and A. Serpette. 2002. [Dynamics and evolution of a northern Meddy. \*J. Phys. Oceanogr.\*, 32, 55–79.](#)
- Paillet, J., B. LeCann, A. Serpette, Y. Morel and X. Carton. 1999. [Real-time tracking of a northern meddy in 1998–98. \*Geophys. Res. Lett.\*, 26, 1877–1880.](#)
- Polvani, L. M. 1988. Geostrophic vortex dynamics, Ph. D. thesis, MIT/WHOI, WHOI-88-48, 221 pp.
- Prater, M. D. 1992. Observations and hypothesized generation of a meddy in the Gulf of Cadiz. PhD thesis, School of Oceanography, University of Washington. Seattle, 131 pp.
- Reinaud, J. N. and D. G. Dritschel. 2002. The merger of vertically offset quasi-geostrophic vortices. *J. Fluid Mech.*, *469*, 287–315.
- . 2005. The critical merger distance between two co-rotating quasi-geostrophic vortices. *J. Fluid Mech.*, *522*, 357–381.
- Richardson, P. L., A. S. Bower and W. Zenk. 1999. Summary of meddies tracked by floats. *International WOCE Newsletter*, N 34, 18–20.
- . 2000. [A census of meddies tracked by floats. \*Prog. Oceanogr.\*, 45, 209–250.](#)
- Richardson, P. L., M. S. McCartney and C. Maillard. 1991. A search for meddies in historical data. *Dyn. Atmos. Oceans*, *15*, 241–265.
- Richardson, P. L. and A. Tychensky. 1998. Meddy trajectories in the Canary Basin measured during the SEMAPHORE experiment 1993–1995. *J. Geophys. Res.*, *103*, C11, 25029–25045.
- Richardson, P. L., D. Walsh, L. Armi, M. Schröder and J. F. Price. 1989. [Tracking three meddies with SOFAR floats. \*J. Phys. Oceanogr.\*, 19, 371–383.](#)
- Schultz Tokos, K., H. H. Hinrichsen and W. Zenk. 1994. [Merging and migration of two meddies. \*J. Phys. Oceanogr.\*, 24, 2129–2141.](#)
- Serra, N., S. Sadux and I. Ambar. 2002. Observations and laboratory modeling of meddy generation at Cape St. Vincent. *J. Phys. Oceanogr.*, *32*, 3–25.

- Shapiro, G. I., S. L. Meschanov and M. V. Emelianov. 1995. Mediterranean lens “Irving” after its collision with seamounts. *Oceanol. Acta*, 18, 309–318.
- Siedler, G., L. Armi and T. J. Müller. 2005. Meddies and decadal changes at the Azores Front from 1980 to 2000. *Deep-Sea Res. II*, 52, 583–604.
- Sokolovskiy, M. A. 1991. Modeling three-layer vortex motions in the ocean by the contour dynamics method. *Izv., Atmos. Oceanic Phys.*, 27, 550–562.
- Sokolovskiy, M. A. and J. Verron. 2000. Finite-core hetons: Stability and interactions. *J. Fluid Mech.*, 423, 127–154.
- Sokolovskiy, M. A., J. Verron and I. M. Vagina. 2001. Effect of a submerged small-height obstacle on the dynamics of a distributed heton. *Izv., Atmos. Oceanic Phys.*, 37, 122–133.
- Spall, M. A., P. L. Richardson and J. Price. 1993. Advection and eddy mixing in the Mediterranean salt tongue. *J. Mar. Res.*, 51, 797–818.
- Stammer, D., H.-H. Hinrichsen and R. H. Käse. 1991. Can meddies be detected by satellite altimetry? *J. Geophys. Res.* 96, 7005–7014.
- Swallow, J. G. 1969. A deep eddy off Cape St. Vincent. *Deep-Sea Res.*, 16, 285–295.
- Takaki, R. and S. G. Kovaznay. 1978. Statistical theory of vortex merger in the two-dimensional mixing layer. *Phys. Fluids*, 21, 153–156.
- Thierry, V. and Y. Morel. 1999. On the influence of a strong bottom slope on the evolution of surface-intensified vortex. *J. Phys. Oceanogr.*, 29, 911–924.
- Tychensky, A. and X. Carton. 1998. Hydrological and dynamical characterization of meddies in the Azores region: a paradigm for baroclinic vortex dynamics. *J. Geophys. Res.*, 103, 25,061–25,079.
- Valcke, S. and J. Verron. 1993a. On interactions between two finite-core hetons. *Phys. Fluids*, A5, 2058–2060.
- 1993b. Interaction of baroclinic isolated vortices: The dominant effect of shielding. *J. Phys. Oceanogr.*, 23, 1346–1362.
- 1996. Cyclon-anticyclon asymmetry in the merging process. *Dyn. Atmos. Oceans.*, 24, 227–236.
- Vandermeirsch, F. O., X. J. Carton and Y. G. Morel. 2003a. Interaction between an eddy and a zonal jet. Part I. One and a half layer model. *Dyn. Atmos. Oceans*, 36, 247–270.
- 2003b. Interaction between an eddy and a zonal jet. Part II. Two and a half layer model. *Dyn. Atmos. Oceans*, 36, 271–296.
- Vandermeirsch, F., Y. Morel and G. Sutyrin. 2001. The net advective effect of a vertically sheared current on a coherent vortex. *J. Phys. Oceanogr.*, 31, 2210–2225.
- 2002. Resistance of a coherent vortex to a vertical shear. *J. Phys. Oceanogr.*, 32, 3089–3100.
- Velasco Fuentes, O. U. 2001. Chaotic advection by two interacting finite-area vortices. *Phys. Fluids*, 13, 901–912.
- Verron, J. and S. Valcke. 1994. Scale-dependent merging of baroclinic vortices. *J. Fluid Mech.*, 264, 81–106.
- Vinogradov, A. S. and Yu. H. Pavel’son. 1980. Thin water stratification on the Sargasso Sea under main thermocline. *Oceanol. Res.*, 16, 591–617 (in Russian).
- Waugh, D. W. 1992. The efficiency of symmetric vortex merger. *Phys. Fluids*, A4, 1745–1758.
- Winant, C. D. and F. K. Browand. 1974. Vortex pairing: the mechanism of turbulent mixing-layer growth at moderate Reynolds number. *J. Fluid Mech.*, 63, 237–255.
- Wüst, G. 1935. Schichtung und zirculation des Atlantischen Ozean. Die Stratosphäre. Exped. “Meteor” 1925-27. *Wiss. Ergebn. Bd 6. T. 1*, 106 pp.
- Yasuda, I. 1995. Geostrophic vortex merger and streamer development in the ocean with special reference to the merger of Kuroshio warm core rings. *J. Phys. Oceanogr.*, 25, 979–996.

- Yasuda, I. and G. R. Flierl. 1995. Two-dimensional asymmetric vortex merger: contour dynamics experiment. *J. Oceanogr.*, *51*, 145–170.
- . 1997. Two-dimensional asymmetric vortex merger: merger dynamics and critical merger distance. *Dyn. Atmos. Oceans*, *26*, 159–181.
- Yegorikhin, V. D., Y. A. Ivanov, V. G. Kort, M. N. Koshlyakov, Y. F. Lukashev, E. G. Morozov, I. M. Ovchinnikov, V. T. Paka, T. B. Tsybaneva, I. F. Shadrin and S. M. Shapovalov. 1987. An intrathermocline lens of Mediterranean water in the tropical North Atlantic. *Oceanology*, *27*, 121–127.

Received: 29 December, 2010; revised: 7 April, 2011.